Capacity of bucket foundation on sand over clay layers

Capacité de la fondation de seau sur sable sur couches d'argile

Duhee Park
Civil and Environmental Engineering, Hanyang University, Korea, dpark@hanyang.ac.kr

Jeong-Seon Park
Civil and Environmental Engineering, Hanyang University, Korea

ABSTRACT: Estimation of base bearing capacity is important in the design of bucket foundations. Empirical formulas for bucket foundations in uniform sand or clay profiles have been proposed. However, the capacity of foundations in alternating layers of sand and clay is not well defined. We perform a series of axisymmetric elasto-plastic finite element analyses on sand layers underlain by clay layers. It is shown that assuming a uniform profile is not appropriate. Even a thin layer of clay below the tip of the bucket foundation can significantly reduce the capacity of the foundation. The wide scatter of results can be significantly reduced through normalization. We present predictive equations and design charts to estimate the base bearing capacity of foundations on heterogeneous profiles.

RÉSUMÉ : L'estimation de la capacité portante est importante dans la conception des fondations de godets. On a proposé des formules empiriques pour des fondations de seaux en sable ou en argile uniforme. Cependant, la capacité des fondations dans des couches alternées de sable et d'argile n'est pas bien définie. Nous réalisons une série d'analyses élasto-plastique en éléments finis axisymétriques sur des couches de sable sous-jacentes à des couches d'argile. Il est montré que l'hypothèse d'un profil uniforme n'est pas appropriée. Même une fine couche d'argile au-dessous de la pointe de la fondation de seau peut réduire considérablement la capacité de la fondation. Nous montrons que la grande dispersion des résultats peut être considérablement réduite par la normalisation. Nous présentons des équations prédictives et des diagrammes de conception pour estimer les capacités portantes des fondations sur des profils hétérogènes.

KEYWORDS: bucket foundation, vertical bearing capacity, alternating layers, finite element analysis

1 INTRODUCTION

Naturally formed soil profiles are usually deposited in layers and are not uniform. An important consideration is the vertical bearing capacity of foundations in sand overlying clay profiles. A series of studies have been performed to calculate and predict the capacity of foundations in sand overlying clay soils. Meyerhof (1974) and Hanna and Meyerhof (1980) assumed that a 'punch-through' failure occurs in the two-layer soil, where the sand block is pushed into the underlying clay. The projected area method, which assumes that the vertical load is spread through the upper sand layer with a projected angle (β) to the underlying clay (Yamaguchi, 1963), has also been used in practice. Okamura et al. (1998) proposed a model that combines the puching shear model and the projected method.

Numerous numerical studies have been performed to evaluate the vertical capacity of strip foundation on sand over clay profiles. Michalowski and Shi (1995) used the upper bound limit analysis to perform parametric studies on strips foundations on sand over clay soil profile. Burd and Frydman (1997) conducted both finite element (FE) and finite difference (FD) methods to predict the bearing capacity of a surface strip foundation resting on sand over clay soil. Shiau et al. (2003) used the upper and lower bound theorems to obtain rigorous plasticity solutions for bearing capacity of strip foundation on sand over clay soil profiles. As summarized, previous researches focus their interests on shallow circular or strip foundations. A predictive method for the bearing capacity of bucket foundations on multi-layered soil profile has not been developed.

In this study, the base bearing capacity of bucket foundations installed in sand overlying clay soils were calculated based on axisymmetric finite element analyses. A parametric study was conducted and the influence of various parameters on the base bearing capacity is investigated. Based on numerical simulations, empirical equations for the base bearing capacity is presented based on regression analyses.

2 FINITE ELEMENT MODEL

Analyses were performed using ABAQUS/Standard (Simulia, 2010). An axisymmetric finite element model was used to conduct a parametric study. In this FE model, the bucket foundation was modeled as a rigid body, prohibiting any relative displacement between the nodes of the elements. We used eight-node biquadratic axisymmetric quadrilateral elements (CAX8) for the soil and foundation.

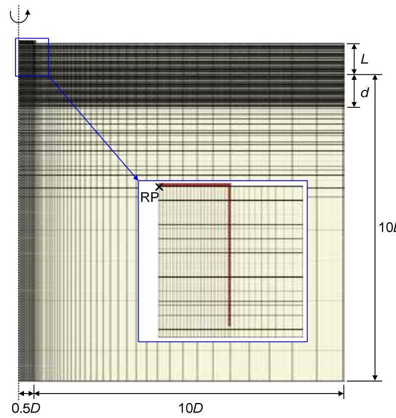

Figure 1. Computation model for the bucket foundation on sand over clay profile.

The bottom of the computational domain was fixed in both horizontal and vertical direction, and the horizontal degree of freedom was fixed at the lateral boundaries. The width of the numerical domain was set to 10.5D from the center of the foundation, and the depth from the tip of the foundation to the bottom of the computational model was set to $10D$. The size of mesh around the bucket foundation was gradually reduced from the boundary towards the center to accurately simulate the changes in stress and strain close to the foundation-soil interface. The length of the smallest element was $0.025D$ (Figure 1).

Linear elastic-perfectly plastic models following Mohr-Coulomb and Tresca failure criteria were used for sands and clays, respectively. An undrained behavior was assumed for the clay layer, whereas sand was assumed to deform in drained condition. To model the interaction between the soil and bucket foundation, we used the interface element implemented in ABAQUS. It was shown that the assumption of a rough interface is adequate for a bucket foundation because the relative deformation of trapped soil within a bucket is limited. On the outer skirt, slip of soil in the tangential direction was allowed using the Coulomb friction model. The interface friction angle (δ) was set to two-thirds of ϕ' of sand.

FE analyses were performed in three steps. In the first step, the geostatic stresses are applied to free-field soil elements. In the second step, the soil elements within the bucket geometry are replaced with foundation elements, and the interface is activated. The installation process of the bucket foundation is not simulated, and foundation is assumed to be “wished-in-place”. The soil properties including density and effective stress maybe altered during installation, especially in the vicinity of the foundation, but it is assumed that it has a minor influence on the calculated bearing capacity. In the last step, the displacement at the top of the foundation is increased until failure is reached.

A total of 320 FE simulations were performed, the matrix of which is summarized in Table 1.

Table 1. Parameters and values performed in the numerical analyses.

L/D	$\phi' - \psi'$	$s_u/\gamma' D$	d/D
0.5	30° - 1°	0.3	0
1	35° - 5°	1	1
1.5	40° - 10°	2	2
2	45° - 15°	4	3
			4

Because bucket foundations are typically installed below the sea level, the submerged unit weight was used. The submerged unit weight of sand (γ') and clay were set to 10 kN/m^3 and 9 kN/m^3, respectively. The Poisson’s ratio (ν) of the clay was fixed to 0.49 to simulate the undrained behavior, and ν of the sand was set to 0.3. The Young’s modulus (E) of sand and clay were set to 200 MPa and 50 MPa. The coefficient of lateral earth pressure at rest (K_o) used were 0.43 and 1 for sand and clay layers, respectively. The elastic properties (E, ν) and K_o values have been reported to have marginal influence on the calculated bearing capacity of the foundation. The soil strength parameters used in the calculations are listed in Table 1. For the parametric study, the friction angle of sand was set to 30°, 35°, 40°, and 45°. Although normally consolidated young sand is expected to have zero cohesion, a small value of cohesion (c = 1 kPa) was applied to enhance the stability of numerical analysis. We used a non-associated flow rule for the Mohr-Coulomb model. The dilatancy angle was calculated as follows:

$$\psi' = \phi' - 30° \tag{1}$$

For the case of ϕ' = 30°, we used ψ' = 1° because ψ' = 0 will cause numerical instability (Loukidis and Salgado, 2009).

The undrained shear strengths used for the clay layer were $s_u/\gamma' D$ = 0.3, 1, 2, and 4.

The diameter (D) and skirt thickness (t) of the bucket foundation model were fixed to 10 m and 0.15 m for all analyses. The skirt length was varied from 5 to 20 m. The aspect ratios of foundations (L/D) modeled were 0.5, 1, 1.5, and 2. The depth from the foundation tip to the clay layer, denoted d, was varied from 0 to $4D$ with an interval of $1D$.

3 VERTICAL BEARING CAPACITY OF BUCKET FOUNDATION

The vertical bearing capacity of a bucket foundation (Q_u) is composed of two factors, which are the base resistance (Q_b) at the tip level and the shaft resistance (Q_s) of the skirt (Hung and Kim, 2012; Park et al., 2016; Yun and Bransby, 2007). In the numerical model, Q_b can be calculated by subtracting the shear resistance acting on the skirt from the total vertical bearing capacity.

Calculated Q_b for all analyses are determined. Results of the calculated q_b (Q_b per unit area) are presented in a dimensionless form Figure 2, which present the results for L/D = 1. The base capacity increases with an increase in d/D, but it is not linearly proportional. After d reaches d_{cri}, the bearing capacity becomes constant. d_{cri} is shown to be dependent on all four parameters considered in this study. d_{cri} increases with ϕ' and decreases with $s_u/\gamma' D$.

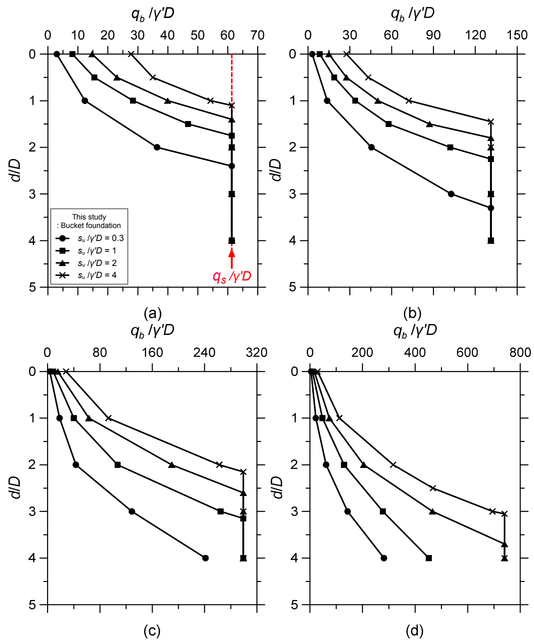

Figure 2. Normalized bearing capacities of bucket foundation (L/D = 1). (a) ϕ' = 30°, (b) ϕ' = 35°, (c) ϕ' = 40°, and (d) ϕ' = 45°.

Increase in L/D causes overburden pressure to increase at sand-clay interface. d/D increases the contribution of the sand layer and also increases the width of the failure surface in the clay layer. ϕ' increases the base capacity in the sand layer, and also causes the failure surface in the clay to widen. For stiff clays, the failure surface is constrained in the overlying sand layer (Figure 3).

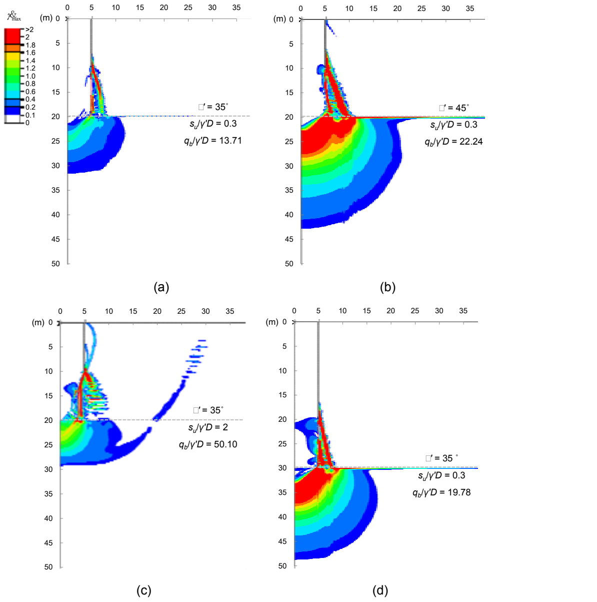

Figure 3. Effect of various parameters on contour of plastic shear strain increment at failure.

$d = 0$ and $d = d_{cri}$ represent the critical cases. For d between two critical cases, the bearing capacity is changed with a function of both the sand and clay capacities. The chart shown in Figure 2 can be used to estimate the bearing capacity. However, they cannot be used beyond the specific parameter values applied in this study.

The base capacity of bucket foundation would be easier to determine if it is represented as follows:

$$q_b = \alpha\, q_s + \varepsilon q_c \tag{2}$$

where α and ε are curve fitting parameters, q_s represents base capacity of bucket foundation in uniform sand, and q_c is capacity for d/D = 0. q_s can be calculated using the bearing capacity equation proposed for bucket foundations in uniform sand (Parket al., 2016). And q_c can be estimated using the equations proposed for bucket foundations in uniform clay.

The base capacity of bucket foundation for d/D = 0 is defined as follows (Hung and Kim, 2012).

$$q_c = s_u N_c s_c d_c \tag{3}$$

$$d_c = 1 + 1.02\left(\frac{L}{D}\right) - 0.42\left(\frac{L}{D}\right)^2 \tag{4}$$

where, N_c = 5.14, and s_c = 1.2, and d_c is depth factor defined as functions of L/D.

After the bearing capacities for q_s and q_c are determined, we calculated the parameters α and ε in Eq. (2), Evaluation of all calculated results revealed that ε is identical to $1-\alpha$. Thus, the equation with two empirical parameters is reduced to a single parameter equation. The calculated values of α for all analyses are summarized in Figure 4. It should be noted that $\alpha = 0$ for d = 0 and $\alpha = 1$ for $d \geq d_{cri}$. α is denoted contribution factor in this study.

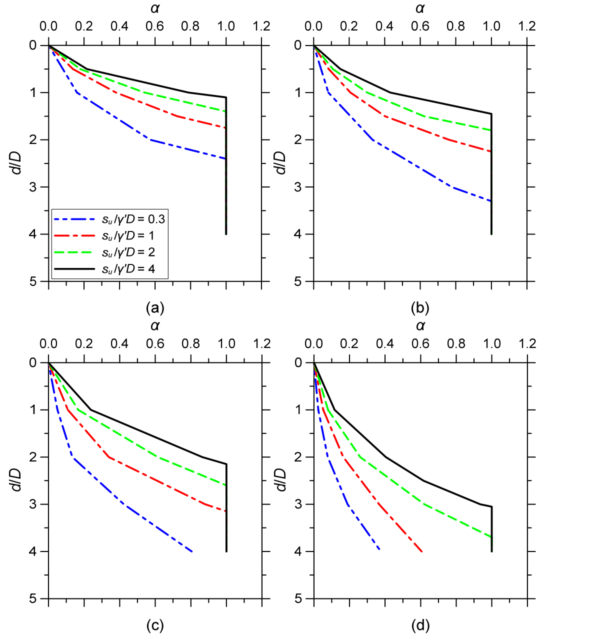

Figure 4. Contribution factors for bearing capacity of bucket foundation (L/D = 1). (a) ϕ' = 30°, (b) ϕ' = 35°, (c) ϕ' = 40°, and (d) ϕ' = 45°.

Close observation of the bearing capacity with depth and α versus depth correlations demonstrate that the shapes and patterns of curves are similar for all cases. Because all curves increase with depth in the form of an exponential function until d_{cri} is reached, d is normalized by d_{cri}. The variation of α with d/d_{cri} are plotted in Figure 5.

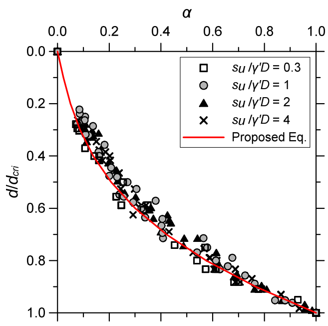

Figure 5. Contribution factor α versus d/d_{cri} relationship.

The results show that all data falls within a narrow bound when normalized. The predictive equation for α is proposed as follows:

$$\alpha = 0.78 \times \left(\frac{d}{d_{cri}}\right)^3 + 0.22 \times \left(\frac{d}{d_{cri}}\right) \tag{5}$$

The equation can be easily used to predict α, once d_{cri} is determined. It was shown that d_{cri} is dependent on L/D, s_u, and ϕ. Statistical analysis was performed to derive the optimum function for d_{cri}. The calculated best-fit function for d_{cri} is the following:

$$\frac{d_{cri}}{D} = 1.44 \times \left(\tan\phi'\right)^{1.75} \times \left(1.84 + 1.1\frac{L}{D}\right) \times \left(\frac{s_u}{\gamma' D}\right)^{-0.31} \tag{6}$$

d_{cri}/D is proportional to ϕ' and L/D, while inversely proportional to $s_u/\gamma' D$. The derived equation and the numerically calculated values for d_{cri} are compared in Figure 6. Comparisons show that the proposed equation agrees very favorably with the results from the numerical analyses.

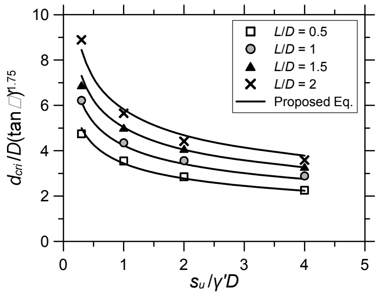

Figure 6. Estimation of critical depth (d_{cri}).

Figure 7 compares the estimated capacities with numerically calculated values. Comparisons highlight that the proposed set of equations provide a reliable estimate of the base capacity.

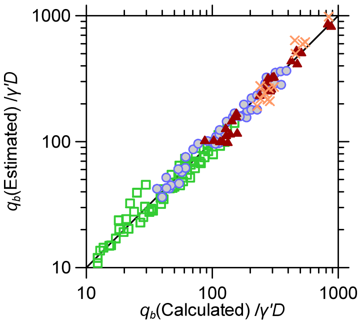

Figure 7. Comparison of calculated and estimated base capacity with the new method.

4 CONCLUSION

The base bearing capacity of bucket foundations installed in sand overlying clay were calculated from finite element analyses. The Mohr-Coulomb model with non-associated flow rule and the Tresca model were used for sands and clays, respectively. A range of aspect ratio (L/D) of bucket foundation and tip-to-clay depth (d) were used.

The strengths of the sand and clay layers are shown to influence the shape of the failure surface both in the sand and clay layers. The shape of foundation and thickness of sand layer are to have important influence on the failure surface and bearing capacity. Design charts and a set of equations to calculate the base capacity based on the numerical results are proposed. Comparisons with the numerical simulations show that the proposed set of equations can accurately predict the base capacity of bucket foundations.

5 ACKNOWLEDGEMENTS

This research was supported by ‘Development of design basis and concrete technologies for offshore wind turbine support structures (20120093)’ funded by the Ministry of Oceans and Fisheries, Republic of Korea.

6 REFERENCE

Burd H.J., and Frydman S. 1997. Bearing capacity of plane-strain footings on layered soils. *Canadian Geotechnical Journal*, 34 (2), 241-253.

Hanna A.M., and Meyerhof G.G. 1980. Design charts for ultimate bearing capacity of foundations on sand overlying soft clay. *Canadian Geotechnical Journal*, 17 (2), 300-303.

Loukidis D., and Salgado R. 2009. Bearing capacity of strip and circular footings in sand using finite elements. *Computers and Geotechnics*, 36 (5), 871-879.

Meyerhof G.G. 1974. Ultimate bearing capacity of footings on sand layer overlying clay. *Canadian Geotechnical Journal*, 11 (2), 223-229.

Michalowski R.L., and Shi L. 1995. Bearing capacity of footings over two-layer foundation soils. *Journal of Geotechnical Engineering*, 121 (5), 421-428.

Park J.S., Park D., and Yoo J.K. 2016. Vertical bearing capacity of bucket foundations in sand. *Ocean Engineering*, 121 (1), 453-461.

Shiau J.S., Lyamin A.V., and Sloan S.W. 2003. Bearing capacity of a sand layer on clay by finite element limit analysis. *Canadian Geotechnical Journal*, 40 (5), 900-915.

Simulia 2010. *Abaqus user’s manual*, Dassault Systèmes Simulia Corp.

Yamaguchi H. 1963. Practical formula of bearing value for two layered ground. *Proceedings of the 2nd ARCMFE*, 99-105.

Yun G., and Bransby M.F. 2007. The undrained vertical bearing capacity of skirted foundations. *SOIL AND FOUNDATIONS*, 47 (3), 493-505.